CHAPTER 4

RESULTS & DISCUSSION

PREPARATION OF $CuAlO_2$ FILMS

Thin films of $CuAlO_2$ were deposited by dc reactive magnetron sputtering on glass substrates under various oxygen partial pressures and substrate temperatures. The deposition parameters maintained during the preparation of the $CuAlO_2$ films are given in the table 4.1.

Table. 4.1: Deposition parameters of $CuAlO_2$ films

Deposition method	:	dc reactive magnetron sputtering
Power source	:	dc power supply (750 V and 3 Amps)
Sputtering target	:	Pure copper-aluminum
Substrates	:	Corning 7059 glass (75 mm x 25 mm x 1mm)
Target to substrate distance	:	65 mm
Ultimate pressure (P_U)	:	$5x10^{-6}$ mbar
Cathode current (I)	:	100 – 300 mA
Sputtering pressure (P_W)	:	$5x10^{-2}$ mbar
Oxygen partial pressure(pO_2)	:	$6x10^{-5} - 5x10^{-3}$ mbar
Substrate temperature	:	303 – 673 K

CHARACTERIZATION OF $CuAlO_2$ FILMS

The deposited $CuAlO_2$ films were characterized by studying the chemical composition, crystallographic structure, electrical and optical properties. The magnetron

sputtered $CuAlO_2$ films were uniform and strongly adherent to the surface of the substrate. The thickness of the films, determined from the optical interference method was in the range 300 – 700nm.

GLOW DISCHARGE CHARACTERISTICS OF COPPER – ALUMINUM ALLOY TARGET

4.1 Dependence of the cathode potential on the oxygen partial pressure

The variations of the cathode potential (copper-aluminum alloy target) with the oxygen partial pressure for different cathode currents are shown in Fig.4.1. The cathode

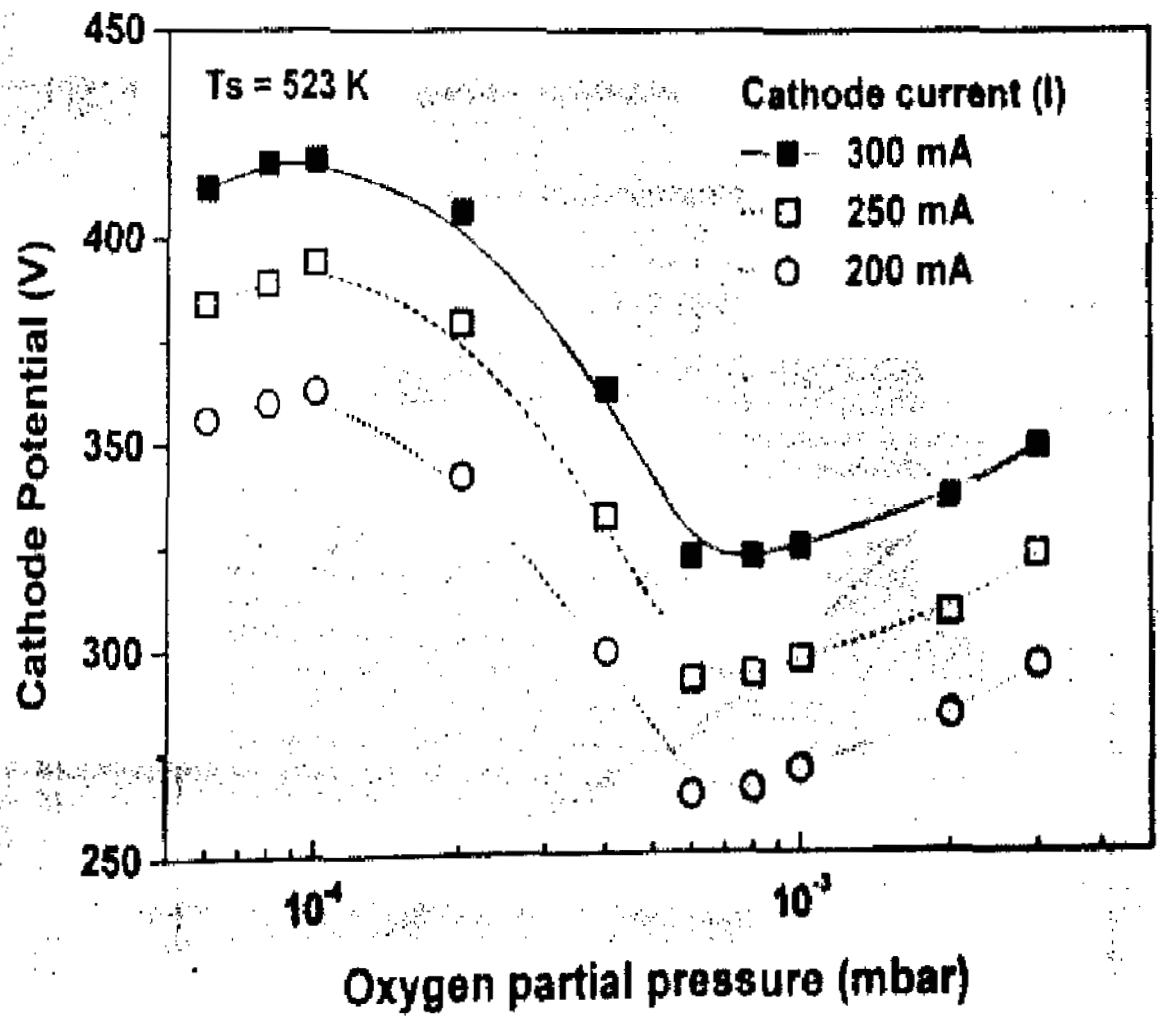

Figure 4.1 Dependence of cathode potential on the oxygen partial pressure of copper-aluminum target

potential initially increased with oxygen partial pressure and gradually decreased and then again increased at higher oxygen partial pressure. The initial increase in the cathode potential is due to the formation of negative oxygen ions. The decrease of cathode potential with further increase of oxygen partial pressure is due to the poisoning of target surface. Further increase of cathode potential with higher oxygen partial pressures was due to the increase of oxide layer thickness on the target surface [1], resulting in the increase of cathode potential. Such a dependence of cathode potential on the oxygen partial pressure was also observed in the sputtering of aluminum [2].

4.2 Dependence of the cathode potential on the substrate temperature

Fig. 4.2 shows the temperature dependence of cathode potential on the copper-aluminum target. At a constant cathode current and oxygen partial pressure

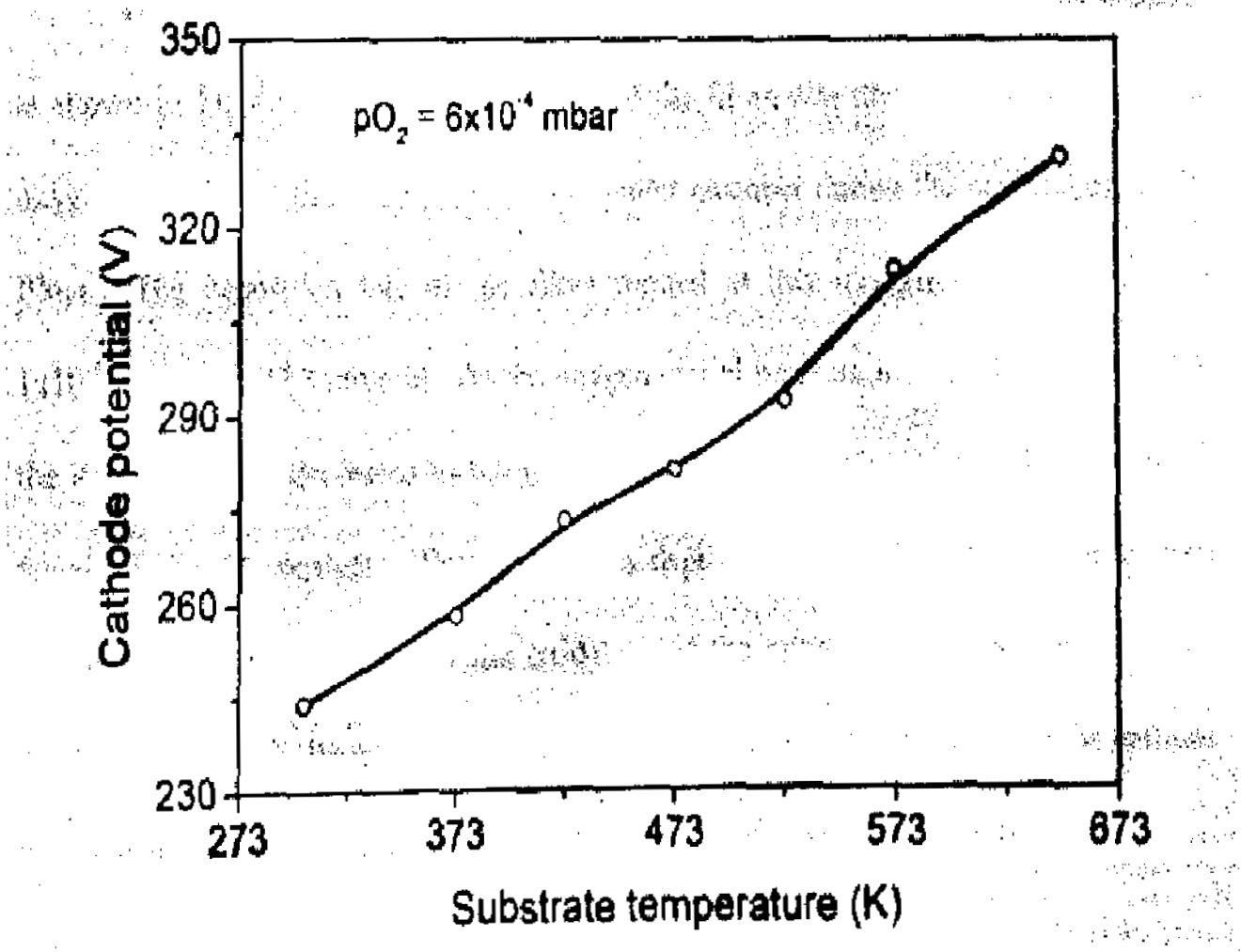

Figure 4.2 Dependence of cathode potential on the substrate temperature

pressure of $6x10^{-4}$ mbar, the cathode potential increased from 244 V to 331 V with the increase of substrate temperature from 373 K to 648 K. As the substrate temperature increased, the plasma state between the target and substrate was changed. At higher substrate temperatures, the temperature of the target surface will also increased due to thermal radiation since the target was kept parallel to the substrate at a distance of 65 mm though the target was cooled with water. Because of this, gas temperature in the plasma volume also changed and influence the plasma parameters like ion density, floating potential and electron density [3] and these effects leads to formation of oxide on the target.

4.3 Dependence of deposition rate on the oxygen partial pressure of $CuAlO_2$ films

The variation of deposition rate of $CuAlO_2$ films with the oxygen partial pressure is shown in Fig.4.3. The deposition rate of the films was directly influenced by the oxygen partial pressure maintained in the sputter chamber during the preparation of the films. The deposition rate of the films formed at low oxygen partial pressure of $1x10^{-4}$ mbar was 27.3 nm/min. As the oxygen partial pressure increased to $1x10^{-3}$ mbar the deposition rate decreased to 6.6 nm/min and at higher oxygen partial pressures it remained almost constant. The decrease in deposition rate with increase of oxygen partial pressure may be due to the oxidation of the sputter target producing of low sputtering yield [4]. It can be seen that the oxygen partial pressure at which the cathode potential starts decrease corresponds to the drop in the deposition rate of the films.

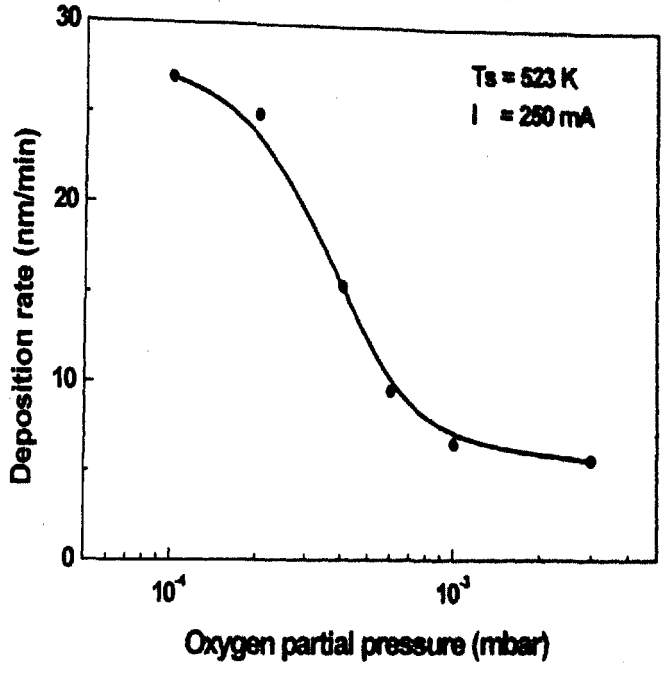

Figure 4.3 Variation of deposition rate of $CuAlO_2$ films with the oxygen partial pressure

4.4 Dependence of deposition rate on the substrate temperature of $CuAlO_2$ films

The substrate temperature also influences the deposition rate (Fig. 4.4.). The deposition rate of the films increased from 2.6 nm/min to 25.67 nm/min with increase of substrate temperature from 303 K to 648 K and remaining almost constant at higher substrate temperatures. The saturation of deposition rate at higher temperature may be due to the reevaporation of the deposited films.

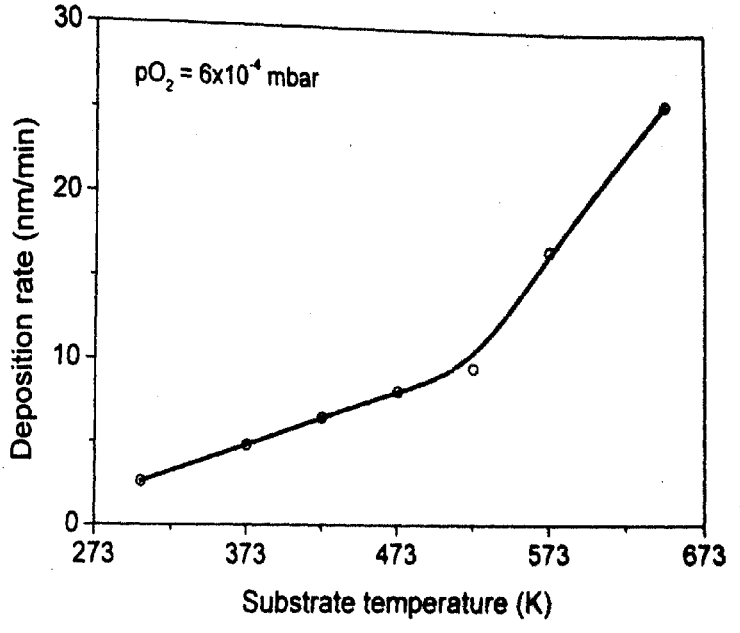

Figure 4.4 Variation of deposition rate of $CuAlO_2$ films with substrate temperature

STRUCTURAL PROPERTIES

4.5 Effect of oxygen partial pressure

The structural studies of the experimental films deposited at various oxygen partial pressures were carried out by X-ray diffraction techniques. Fig.4.5 shows the X-ray diffraction spectra of $CuAlO_2$ films formed at different oxygen partial pressures. The diffraction profiles indicated that the films were polycrystalline in nature. The films formed at an oxygen partial pressure of $2x10^{-4}$ mbar showed two peaks at 2θ of 31.53° and 36.34° corresponding to the presence of (006) planes of $CuAlO_2$ and (111) planes of Cu_2O respectively. When the oxygen partial pressure increased to $6x10^{-4}$ mbar the peak

related to the Cu_2O disappeared and additional peaks were observed at 2θ = 15.61°, 37.66°, 48.29° and 65.51° identified as (003), (012), (009) and (110) along with (006) planes of $CuAlO_2$, indicating that the films were Rhombohedral structure with space group of R3m and is in good agreement with the standard data [JCPDS. No 09 –0185]. The intensity of the peaks increased with the increase of oxygen partial pressure. The films formed at higher oxygen partial pressures (>$6x10^{-4}$ mbar) exhibited an additional

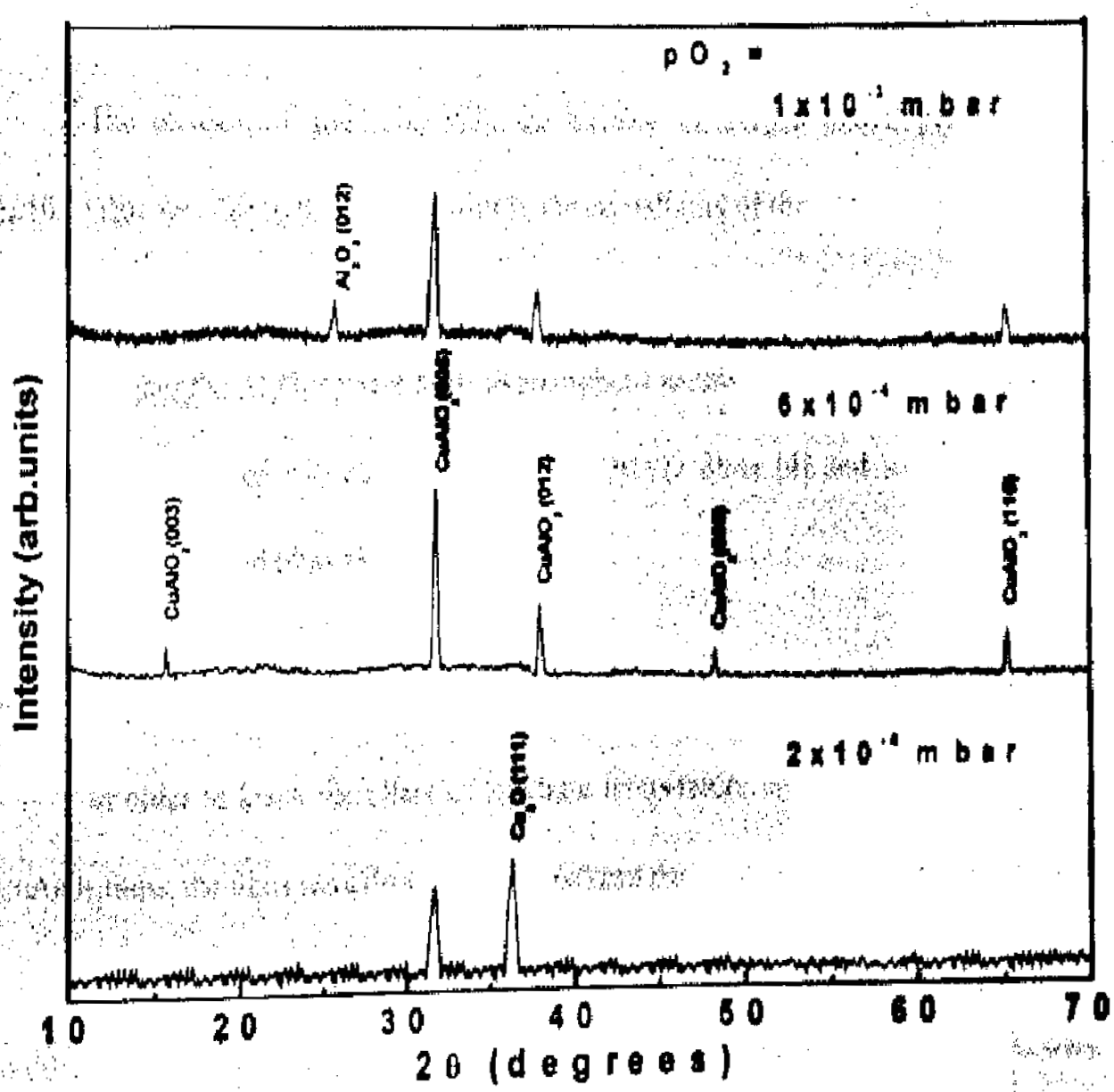

Figure 4.5 X-ray diffraction patterns of $CuAlO_2$ films at different oxygen partial pressures

peak at 2θ =25.65° related to the (012) plane of Al_2O_3 phase along with $CuAlO_2$. It was also observed that the intensity of peaks decreased with the increase of oxygen partial pressure and also the (009) plane and (003) plane of $CuAlO_2$ were disappeared. From these studies it revealed that single phase films of $CuAlO_2$ were obtained at an oxygen partial pressure of $6x10^{-4}$ mbar. The grain size of the films increased from 10 nm to 35 nm with the increase of oxygen partial pressure from $2x10^{-4}$ mbar to $6x10^{-4}$ mbar beyond which, it decreased to 15 nm at higher oxygen partial pressure of $1x10^{-3}$ mbar.

The increase of grain size with the increase of oxygen partial pressure upto $6x10^{-4}$ mbar was due to the improvement in the crystallinity of the films. The decrease in the grain size at oxygen partial pressures > $6x10^{-4}$ mbar may be due to the presence of Al_2O_3. Higher the Al_2O_3 content leads to amorphous nature of the films. The grain size of the films obtained was comparable to pe-MOCVD films [4] and smaller than the pulsed laser deposited films [5].

4.6 Effect of substrate temperature

In order to know the effect of substrate temperature on structural properties of $CuAlO_2$ films, the films were deposited at an oxygen partial pressure of $6x10^{-4}$ mbar with different substrate temperatures. The X-ray diffraction spectra of $CuAlO_2$ films formed at different substrate temperature is shown in Fig.4.6. The films formed at 303 K were amorphous in nature. The amorphous nature of the films formed at low substrate temperature was due to insufficient thermal energy for the diffusion of adatoms on the substrate surface for the nucleation. The films formed at 373 K were polycrystalline in nature with (006) phase of $CuAlO_2$. As the substrate temperature increased, the

crystallinity of the films increased. The films formed at a substrate temperature of 523 K showed four additional peaks at 2θ = 15.61°, 37.66°, 48.29° and 65.51° identified as (003), (012), (009) and (110) along with (006) planes of $CuAlO_2$ exhibits Rhombohedral structure with R3m space group. The intensity of (006) and (012) increased and suppressed other peaks with further increase of substrate temperature. The films exhibited only two peaks corresponding to (006) and (012) orientation when the films formed at higher substrate temperature of 648 K.

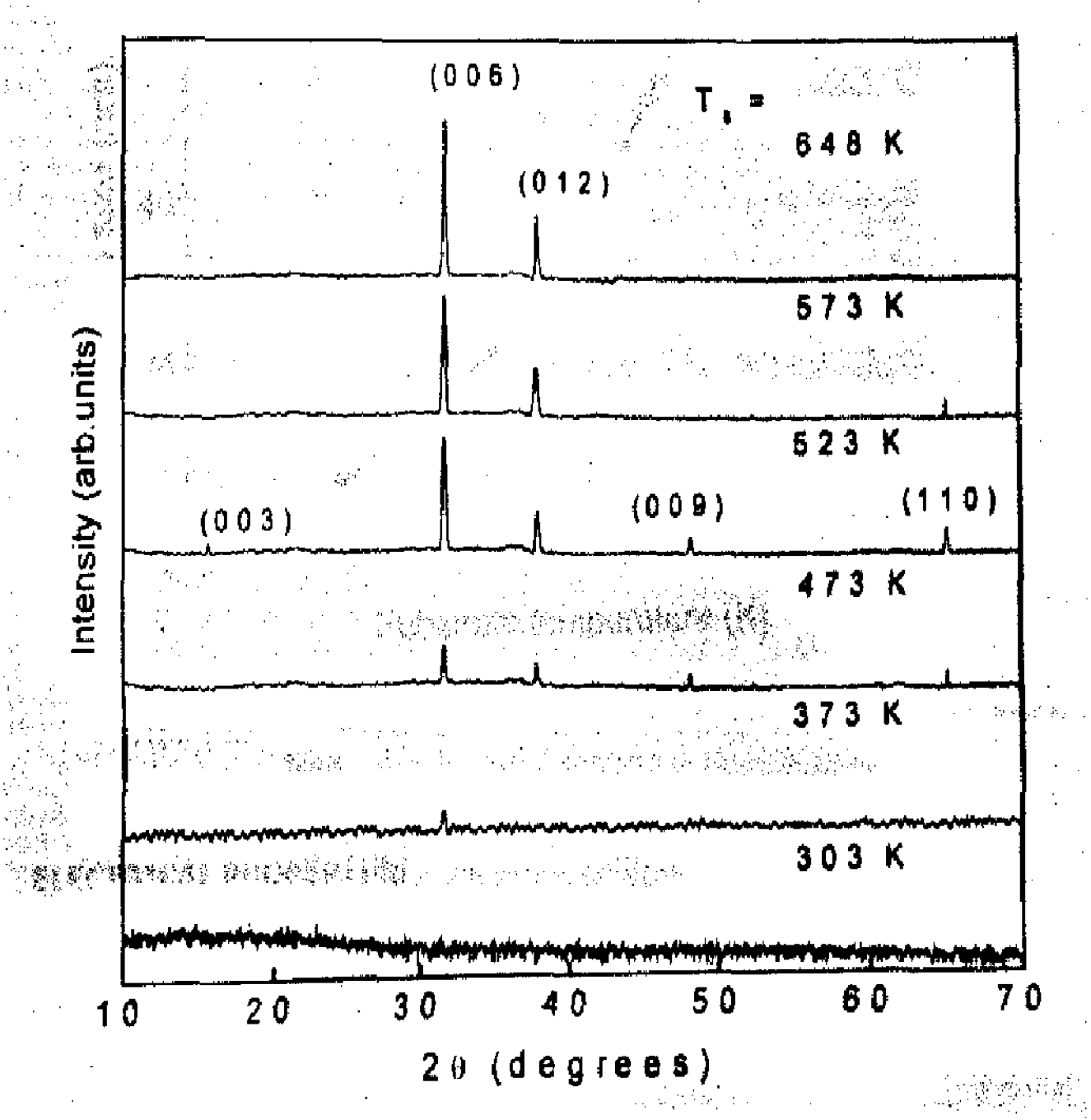

Figure 4.6 X-ray diffraction patterns of $CuAlO_2$ films formed at different substrate temperatures

The variation of grain size with substrate temperature is shown in Fig.4.7. The grain size of the films increased from 14 nm to 68 nm with the increase of substrate temperature from 373 K to 648 K, which was due to the improvement in the crystallinity of the films.

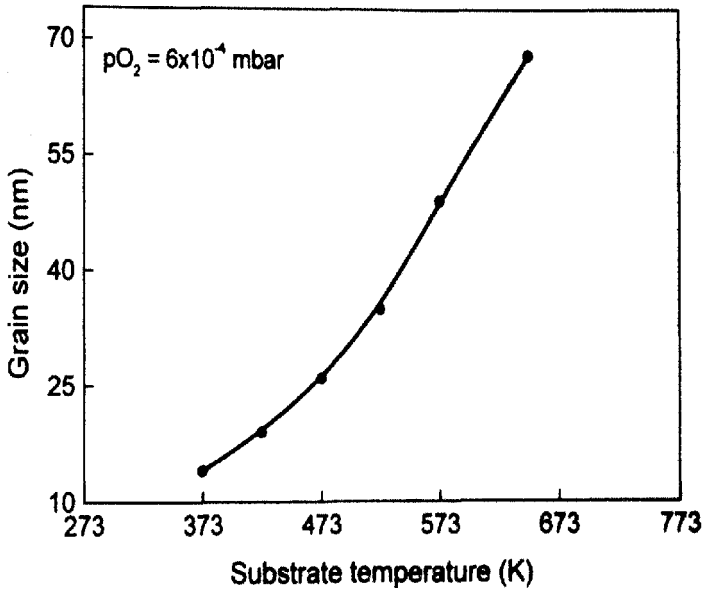

Figure 4.7 Dependence of grain size on the substrate temperature of $CuAlO_2$ films

ELECTRICAL PROPERTIES

4.7 Effect of oxygen partial pressure

The electrical properties of the films were highly influenced by the oxygen partial pressure. Fig.4.8 shows the electrical resistivity (ρ), Hall mobility(μ) and carrier concentration (n) of $CuAlO_2$ films formed at different oxygen partial pressures. At low

oxygen partial pressures ($1x10^{-4}$ mbar), due to the presence of mixed phases of Cu_2O and $CuAlO_2$, the films exhibited high electrical resistivity of 15.2 Ωcm. The electrical resistivity of the films decreased with increasing oxygen partial pressure. Low electrical resistivity of 3.1 Ωcm was observed when the films deposited at an oxygen partial pressure of $6x10^{-4}$ mbar, which was due to growth of single phase of $CuAlO_2$. Further increase in the oxygen partial pressure to $1x10^{-3}$ mbar, the electrical resistivity increased to 18.9 Ωcm due to the formation of Al_2O_3 phase along with $CuAlO_2$. Higher

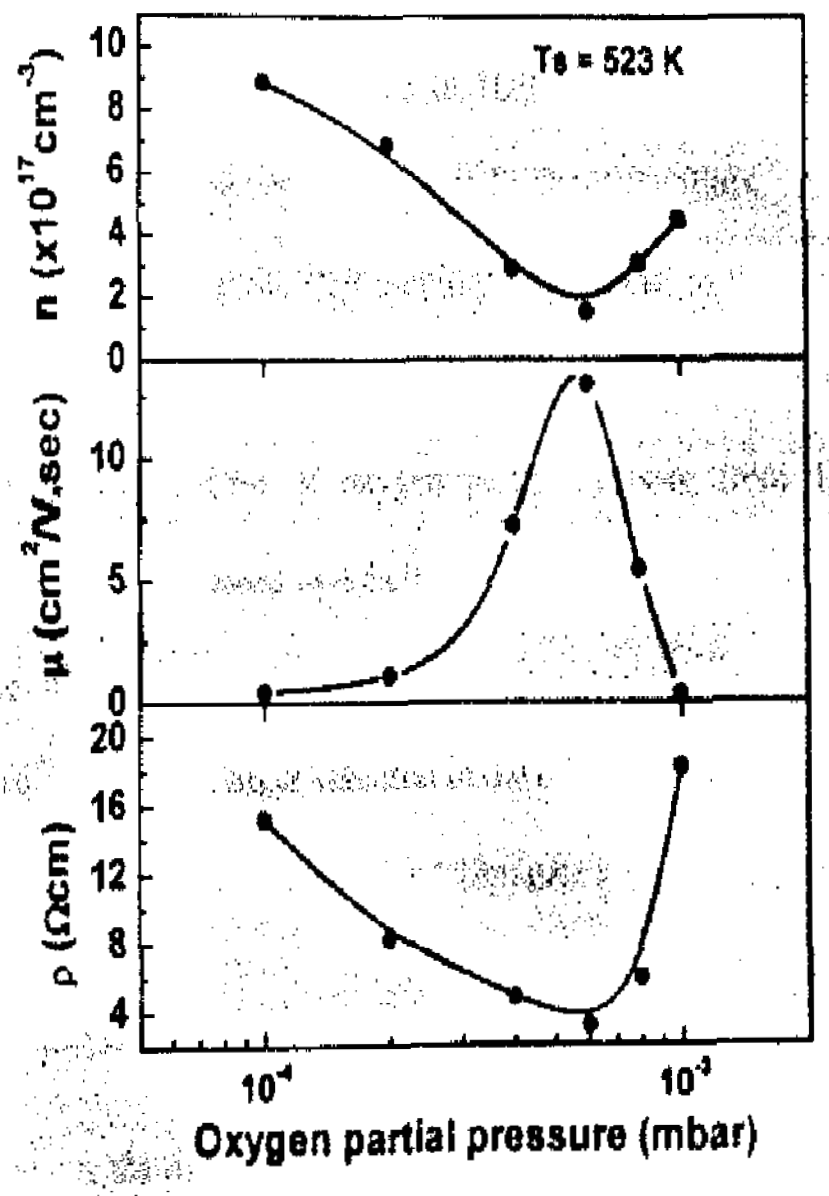

Figure 4.8 Variation of electrical resistivity (ρ), Hall mobility (μ) and carrier concentration (n) of $CuAlO_2$ films

the content of Al_2O_3 in the films leads to dielectric behaviour and amorphous nature, hence of high electrical resistivity. The low electrical resistivity of 3.1 Ωcm obtained was lower than 10.5 Ωcm, which was reported in pulsed laser deposition [5] and 12 Ωcm obtained in dc sputtered films [6]. Wang and Gong [7] achieved low electrical resistivity of 0.14 Ωcm in plasma enhanced MOCVD due high carrier concentration of $4.5x10^{19}$ cm^{-3}. The Hall mobility measurements indicated that the films were p-type in conduction. The Hall mobility of the films increased from 0.5 $cm^2/Vsec$ to 13.1 $cm^2/Vsec$ with increasing the oxygen partial pressure up to $6x10^{-4}$ mbar thereafter it decreased to 0.25 $cm^2/Vsec$. The increase of Hall mobility with the oxygen partial pressure was due to the improvement in the crystallinity of the films. At higher oxygen partial pressures the decrease in the Hall mobility may be due to the presence of Al_2O_3 phase. The carrier concentration of the films decreased from $8.9x10^{17}$ cm^{-3} to $1.5x10^{17}$ cm^{-3} with the increase of oxygen partial pressure from $1x10^{-4}$ mbar to $6x10^{-4}$ mbar thereafter, it increased to $4.5x10^{17}$ cm^{-3} at higher oxygen partial pressures. In the literature it was reported that the carrier concentration was in the range $1.3x10^{17} - 4.5x10^{19}$ cm^{-3}. The larger variation in the carrier concentration was due to the preparation of films using different deposition techniques and process parameters.

4.8 Effect of substrate temperature

Fig. 4.9 shows the dependence of electrical resistivity (ρ), Hall mobility(μ) and carrier concentration (n) of $CuAlO_2$ films formed at different substrate temperatures. The electrical properties of the films were highly influenced by the substrate temperature. The films exhibited high electrical resistivity at low temperatures due to the amorphous

nature. The electrical resistivity of the films decreased from 17.1 Ωcm to 1.1 Ωcm with the increase of substrate temperature from 373 K to 648 K. The decrease in electrical resistivity with increase of substrate temperature may due to the improvement of crystallinity. The Hall mobility of the films increased from 4.2 cm^2/Vsec to 30.3 cm^2/Vsec with increase of substrate temperature from 373 K to 648 K. The carrier concentration of the films increased from $8.1x10^{16}$ cm^{-3} to $1.9x10^{17}$ cm^{-3} with the increase of substrate temperature from 373 K to 648 K. The increase of carrier mobility and concentration may be due to the improvement in the grain size and hence decrease in the

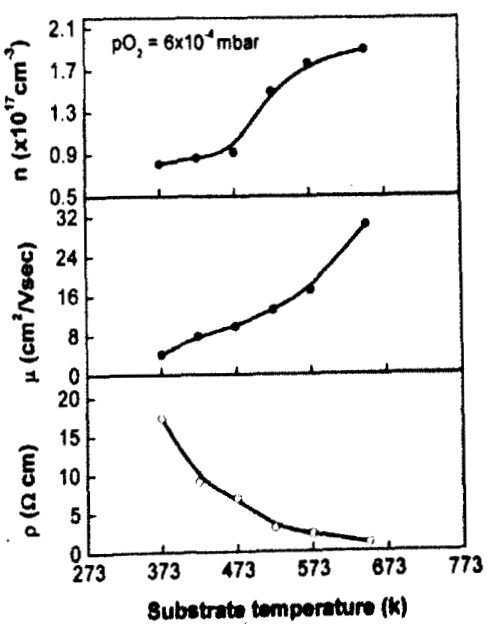

Figure 4.9 Variation of electrical resistivity (ρ), Hall mobility (μ) and carrier concentration (n) with the substrate temperature of $CuAlO_2$ films

grain boundary, which minimizes the trapping and / or scattering of charge carriers at the grain boundaries. The observed carrier nobilities of the films are lower than the bulk due to the presence of oxygen vacancies and / or excess metal interstitial atoms.

OPTICAL PROPERTIES

4.9 Influence of oxygen partial pressure

The optical transmittance and reflectance of the films were recorded in the wavelength range 350 – 2500 nm. Fig.4.10 shows the wavelength dependence of optical transmittance of $CuAlO_2$ films formed at different oxygen partial pressures. The optical

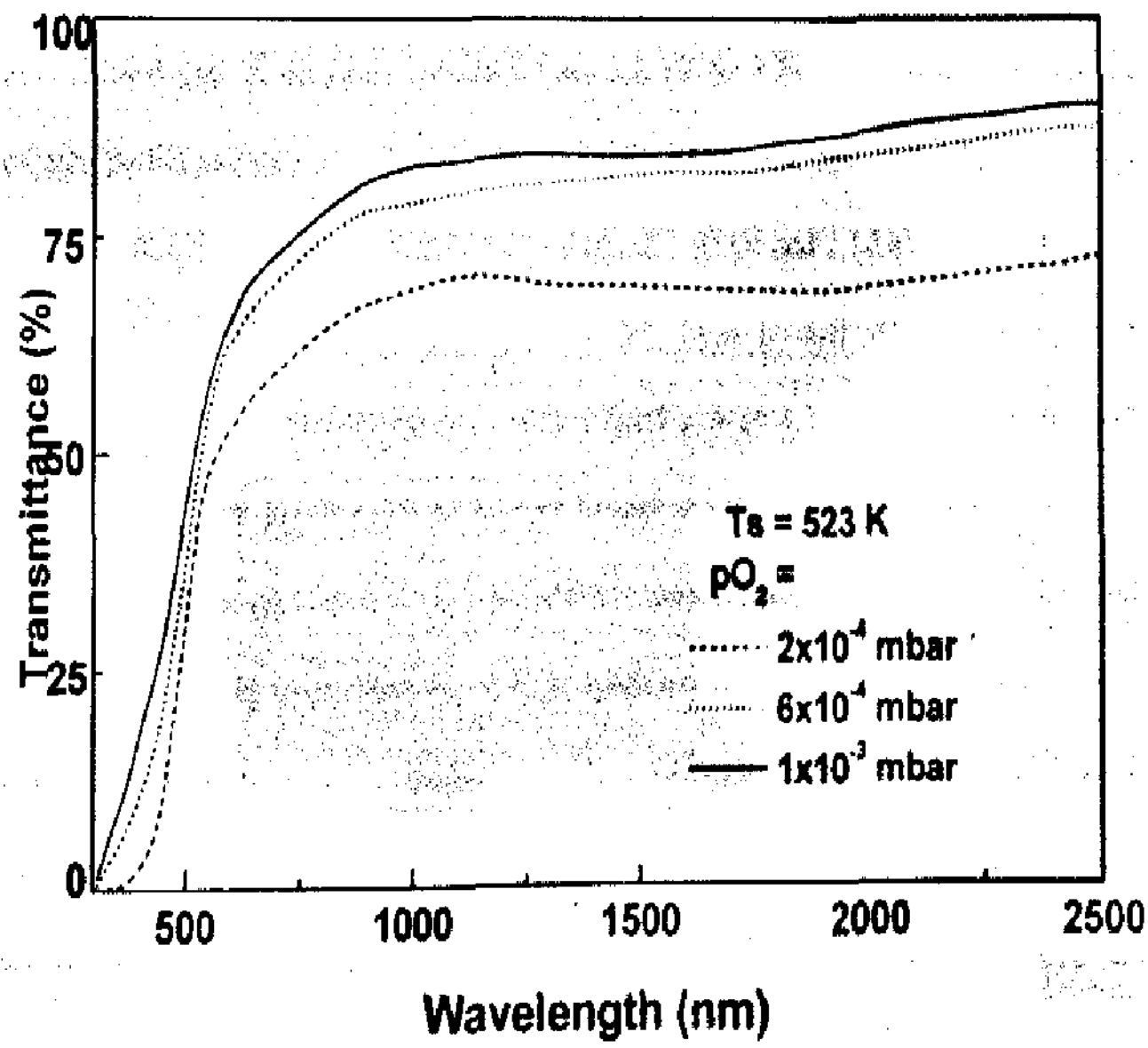

Figure 4.10 Optical transmittance spectra of $CuAlO_2$ films

transmittance is high in the visible region. The low optical transmittance at oxygen partial pressures < $6x10^{-4}$ mbar was due to the presence of insufficient oxygen during sputtering, hence the presence of mixed phase of Cu_2O and $CuAlO_2$. As the oxygen partial pressure increased to ≥ $6x10^{-4}$ mbar the stoichiometry improved because of the decrease in the density of defect centers in the films. The light scattered by the process of reflection decreased with the decrease of defect centers, hence increase in the optical transmittance. The optical transmittance at wavelengths greater than 700 nm increased from 56 % to 76 % with the increase of oxygen partial pressure from $1x10^{-4}$ mbar to $3x10^{-3}$ mbar. A sharp absorption edge was observed around the wavelength 500 nm and shifted towards lower wavelength with the increase of oxygen partial pressure. The optical band gap of the films increased from 3.1 eV to 3.73 eV with the increase of oxygen partial pressure from $2x10^{-4}$ mbar to $1x10^{-3}$ mbar. The optical band gap was not matched with the reported CuO and Cu_2O values of 1.50 eV and 2.10 eV [8,9] and Al_2O_3 value of 9.0 eV [10]. The single phase $CuAlO_2$ films formed at an oxygen partial pressure of $6x10^{-4}$ mbar exhibited an optical band gap of 3.54 eV, which is in good agreement with the reports of Brus [11] and Yanagi et al [12]. However in the literature large optical band gaps of 3.75 eV and 3.66 eV were reported by Gong et al [13] and Banerjee et al [14] in pe-MOCVD and dc sputtered films respectively. This wider optical band gap was caused by quantum confinement because the excitation confinement in semiconductor nanocrystals leads to the development of discrete transitions to the excited electronic states with higher oscillator strength and to band gaps that increase as an inverse function of crystallite size [15-16].

4.10 Figure of merit

The quality of a transparent conducting oxide will be judged by the parameter of figure of merit. The variation in the figure of merit of $CuAlO_2$ with different oxygen partial pressures is shown in Fig.4.11. Figure of merit of the films increased from 0.11 $\Omega^{-1}cm^{-1}$ to 0.87 $\Omega^{-1}cm^{-1}$ with increase of oxygen partial pressure from $1x10^{-4}$ mbar to $6x10^{-4}$ mbar afterwards it decrease to 0.17 $\Omega^{-1}cm^{-1}$ with further increasing the oxygen partial pressure. The increase of figure of merit at lower oxygen partial pressure was due to the decrease in the electrical resistivity. The decrease at higher oxygen partial pressure was due to the increase of electrical resistivity though the films showed high optical transmittance.

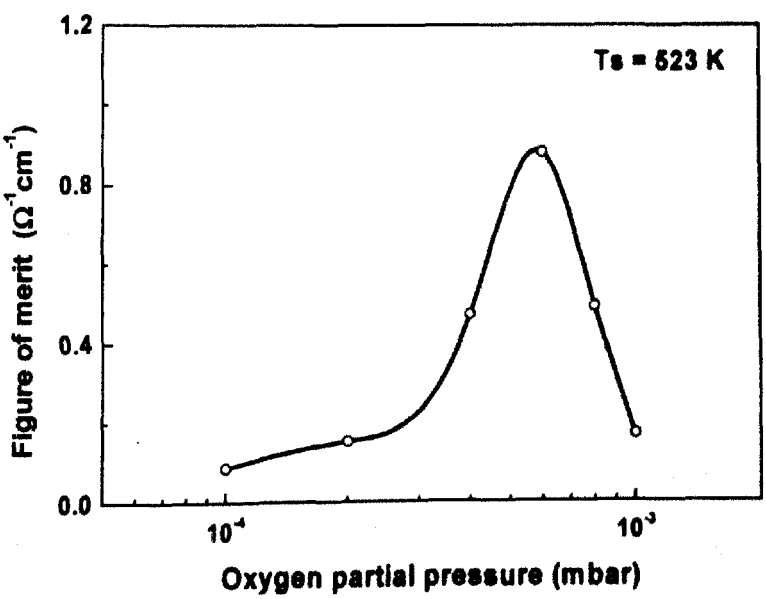

Figure 4.11 Dependance of figure of merit on the oxygen partial pressure of $CuAlO_2$ film

4.11 Effect of substrate temperature

Fig.4.12 shows the wavelength dependence of optical transmittance of $CuAlO_2$ films formed at different substrate temperatures. The optical transmittance of the films decreased from 83 % to 60 % with increase of substrate temperature from 373 K to 648 K. The decrease of the transmittance with increase of substrate temperature was

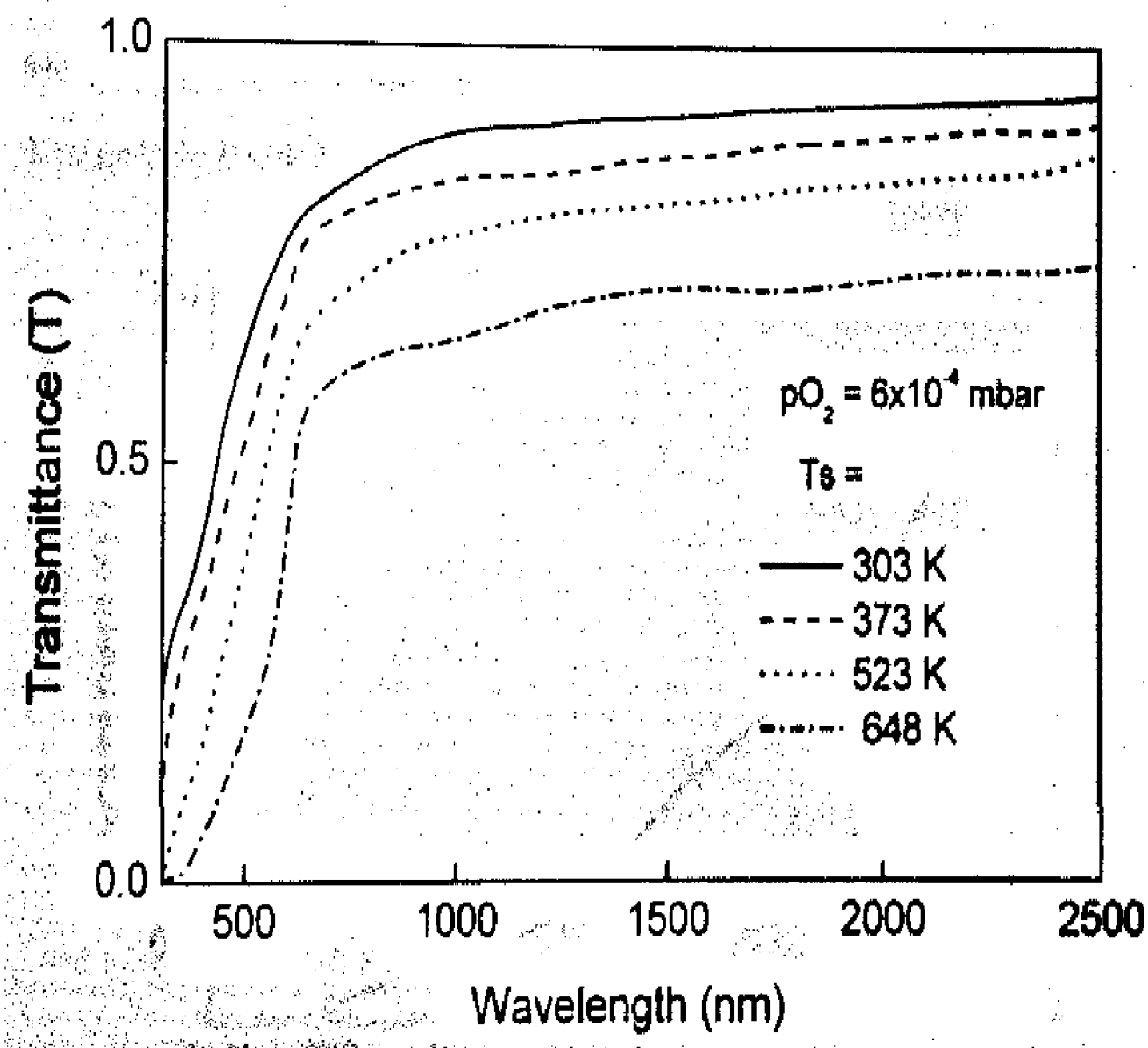

Figure 4.12 Optical transmittance spectra of $CuAlO_2$ films

due to the oxygen deficiency at higher substrate temperatures. The optical band gap of the films decreased from 3.87 eV to 3.11 eV with the increase of substrate temperature from 373 K to 648 K. The single phase $CuAlO_2$ films formed at substrate temperature

of 523 K exhibited an optical band gap of 3.54 eV. In the literature large optical band gap of 3.96 eV was reported by Kim in electron beam evaporation.

4.12 Figure of merit

The variation in the figure of merit of $CuAlO_2$ with different substrate temperatures partial pressure is shown in Fig.4.13. Figure of merit of the films increased from 0.245 $\Omega^{-1}cm^{-1}$ to 1.779 $\Omega^{-1}cm^{-1}$ with increasing substrate temperate from 373 K to 648 K. The increase of figure of merit with substrate temperature was due to the decrease in the electrical resistivity.

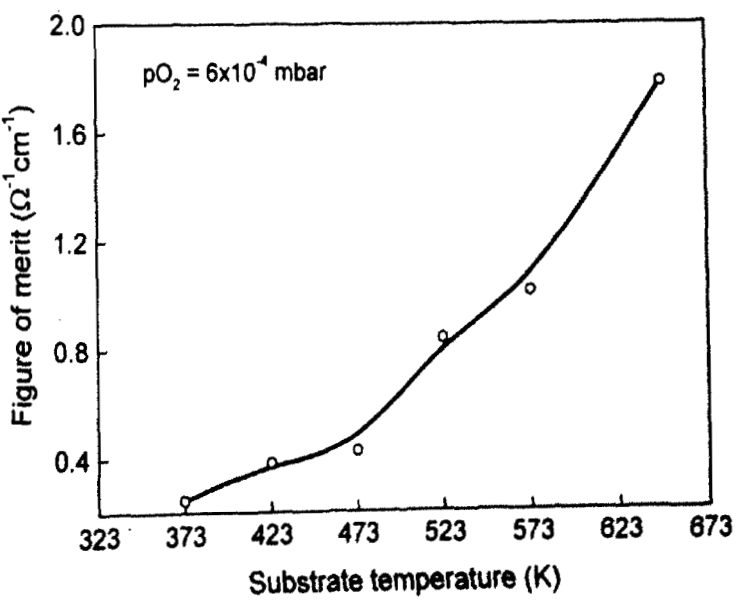

Figure 4.13 Dependence of figure of merit on the substrate temperature of $CuAlO_2$ films

From the present investigation, it was observed that the present study, the $CuAlO_2$ films formed at an oxygen partial pressure of $6x10^{-4}$ mbar and at a substrate temperature of 523 K were Rhombohedral structure with space group of R3m and exhibited electrical resistivity of 3.1 Ωcm, Hall mobility of 13.7 $cm^2/Vsec$, optical transmittance of 71 % with an energy gap of 3.54 eV and figure of merit of 0.87 $\Omega^{-1}cm^{-1}$.

References

[1] G. Mohan Rao and S. Mohan
J. Appl. Phys., 69 (1991) 6652.

[2] W.D. Sproul, D.J. Chistie and D.C. Carter
Thin Solid Films, 491 (2005) 1.

[3] J. Morales, L. Sanchez, S. Bijani, L. Martinez, M. Gabas and F.R. Ramos-Barrado Electochem. Solid State. Lett. 8, (2005) A159

[4] K.B. Sundaram and A. Khan
Thin Solid Films, 295 (1997) 87.

[5] H. Kawazoe, M. Yasukawa, H. Hyodo, M. Kurita, H. Yanagi and H. Hosono
Nature, 389 (1997) 939.

[6] A.N. Banerjee, C.K. Ghosh and K.K. Chattopadhyay
Solar Energy Mater.& Solar Cells, 89 (2005) 75.

[7] Y. Wang and H. Gong
Chemical Vapor Deposition, 6 (2000) 285.

[8] B. Balamurugan and B.R. Mehta
Thin Solid Films, 396 (2001) 90.

[9] A. Buljan, M. Llunell, E. Ruiz, P. Alemany
Chem. Mater.,13 (2001) 338.

[10] M. Henyk, D. Wolfframm and J. Reif
Appl. Surf. Sci., 168 (2000) 263.

[11] L. Brus
J. Chem. Phys., 80 (1984) 4403.

[12] H. Yanagi, S. Inoue, K. Ueda, H. Kawazoe and H. Hosono
J. Appl. Phys., 88 (2000) 4159.

[13] H. Gong, Y. Wang and Y. Luo
Appl. Phys. Lett., 76 (2000) 3959.

[14] A.N. Banerjee, R. Maity, C.K. Ghosh and K.K. Chattopadhyay
Thin Solid Films, 440 (2003) 5 and 474 (2005) 261.

[15] J.R. Heath
Science, 270 (1995) 1315.

[16] Z.H. Lu, D.J. Lockwood and J.M. Baribeau
Nature, 378 (1995) 258.

[17] D.S. Kim and S.Y. Choi
Phys. Stat. Solidi (a), 202 (2005) R 167.